Mine Water Environ (2018) 37:300–311
DOI 10.1007/s10230-017-0500-2

TECHNICAL ARTICLE

Prevention of Groundwater Disasters in Coal Seam Floors Based on TEM of Cambrian Limestone

Qi Wang[1] · Xinyi Wang[2,3,4] · Xiaoman Liu[2] · Xiaoge Zhen[2] · Jianwei Guo[3] · Guosheng Chen[3] · Bo Zhang[3]

Received: 2 January 2017 / Accepted: 1 November 2017 / Published online: 10 November 2017

Abstract We analyzed the abundance and connectivity of Cambrian limestone aquifers (CL) using data from geological and hydrogeological boreholes, groundwater tracer tests, groundwater temperature monitoring, and surface transient electromagnetic exploration (TEM). Our results demonstrate that extremely well-developed small faults with an average density of number 73 per square km control the groundwater abundance and flow of the CL. The hydraulic conductivity of the CL aquifers estimated by tracer tests lies between 13,511 and 38,738 m/d, suggesting good connectivity. The surface TEM result of 4.91 km^2 shows that areas with an apparent resistivity value less than 30 Ωm can be treated as an anomalous low-resistivity zone. This has been proven to be reliable by experience at the working face and can be used to determine water control measures for future mining. Using these data, we developed a series of preventive measures to mitigate potential floor water ingress related to future mining in the eastern area of the Pingdingshan coalfield No. 2 mine.

Keywords Aquifer abundance · Connectivity · Transient electromagnetic exploration

✉ Xinyi Wang
wangxy@hpu.edu.cn

Qi Wang
wangqi@ncwu.edu.cn

[1] School of Resources and Environment, North China University of Water Resources and Electric Power, Zhengzhou 450045, China

[2] Institute of Resources and Environment, Henan Polytechnic University, Jiaozuo 454000, China

[3] Institute of Energy and Chemical Industry of China Pingmei Shenma Group, Pingdingshan 467000, China

[4] Collaborative Innovation Center of Coalbed Methane and Shale Gas for Central Plains Economic Region, Jiaozuo 454000, Henan Province, China

Introduction

Throughout the North China coalfield (NCC), Ordovician or Cambrian limestone (CL) aquifers beneath coal seams are characterized by well-developed karst features, large water-bearing capacity, good connectivity, and high water pressures (Jing et al. 2014; Zhang et al. 2012), which not only increase mine water inflow, but also pose tremendous threats to deep coal mining. For example, a water inrush from an Ordovician limestone that occurred in the Zhaogezhuang Mine had a maximum inflow rate of 123,180 m^3/h, which flooded the mine and caused a number of casualties and severe economic losses (Sun et al. 2015). Thus, it is important to study groundwater connectivity in the thick Ordovician or CL aquifers, as this research has the potential to prevent future inrush events.

In addition, coal mining can affect the recharge, flow, and discharge of groundwater in the NCC differently, depending on whether the water is sourced from the Ordovician or CL groundwater, which in turn affects urban and rural water supply (Howladar et al. 2017; Yin et al. 2016).

Many exploration methods are used to analyze the abundance and connectivity of limestone aquifers beneath coal seams (Andrea et al. 2016; Attila et al. 2015; Lambán et al. 2015; Shi and Wu 2011). Methods for prevention of limestone water ingress include: blocking channels of ground recharge and groundwater runoff, reinforcing aquicludes via grouting, designing and retaining waterproof coal pillars, constructing waterproof gates and mine discharge systems, and draining and decompressing groundwater (Anandan et al. 2010; Wang et al. 2017).

This is an urgent problem and researchers are interested in solving the role of prevention and control of water hazards from the coal floor in the NCC, such as the reliable delineation of an aquifer abundance area, the accurate identification of groundwater connectivity, the accurate detection of transient electromagnetic, and the effective implementation of control plan (Huang and Chen 2012; Wu et al. 2013; Yin et al. 2015). Based on the data obtained by comprehensive exploration technology, this paper analyzes the abundance and groundwater connectivity of the CL aquifers, and corresponding measures to control water damage in the No. 2 mine of the Pingdingshan coalfield, which is located in the NCC area.

Regional Hydrogeological Conditions

The Pingdingshan coalfield has an area of about 650 km^2 (Fig. 1). At present, mainly the Permian Shanxi Formation 2_1 and the Carboniferous 1_5 seams are mined (Fig. 2), and the principle water hazard comes from the CL aquifers. The CL burial depth is between 0 and 1,467.5 m (Fig. 1) in this coalfield. In the southwestern part of the coalfield, the CL is exposed with zonal distribution. The buried depth near the Zhugemiao anticline is between 26.5 and 50 m. The CL depth of the northwest part in the No.13 Mine is less than 100 m.

In the exposed area of the CL, the groundwater is recharged annually by precipitation and surface water. In the area where the aquifers are buried (Fig. 1), the groundwater is also recharged by groundwater from the overlying unconsolidated Quaternary aquifers.

The CL groundwater level elevation is between − 200 m to − 550 m, higher in the southwest and lower in the northeast. Runoff from the CL flows downgradient, predominantly in a northeastern direction (Fig. 1). The groundwater discharge is dominantly mine drainage; the drainage flow in the Pingdingshan coalfield is about 5000 m^3/h.

The Characteristics of Mine Water Filling

Layout of the No. 2 Mine.

The No. 2 mine is divided into western and eastern areas by the Geng3 main haulage road (Fig. 3), and the 1.6 m thick 1_5 coal seam of the Carboniferous Taiyuan Formation is the major target (Fig. 2). From June 2012 through the end of 2020, this seam will be mined mainly in the eastern areas

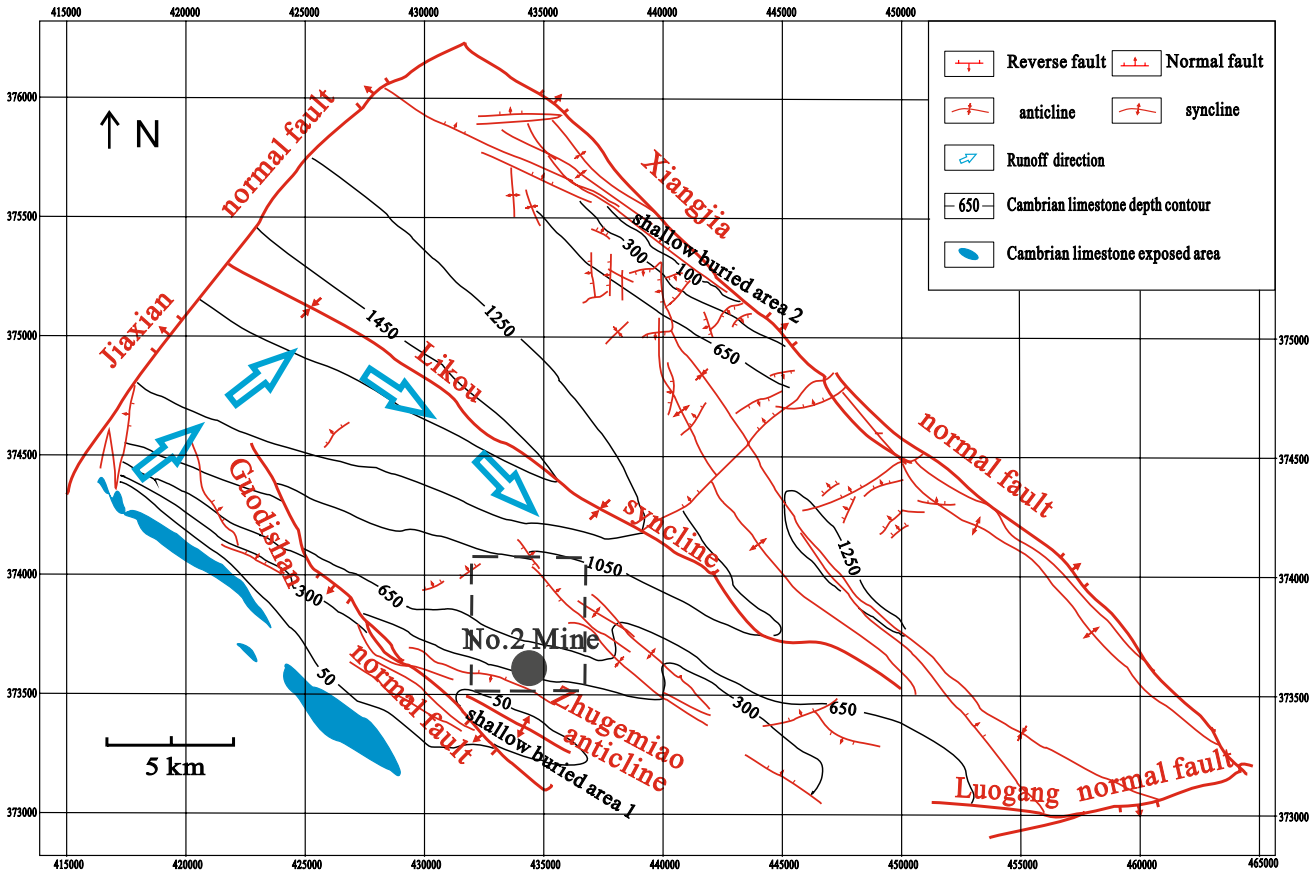

Fig. 1 Buried depth distribution of the CL in Pingdingshan coalfield

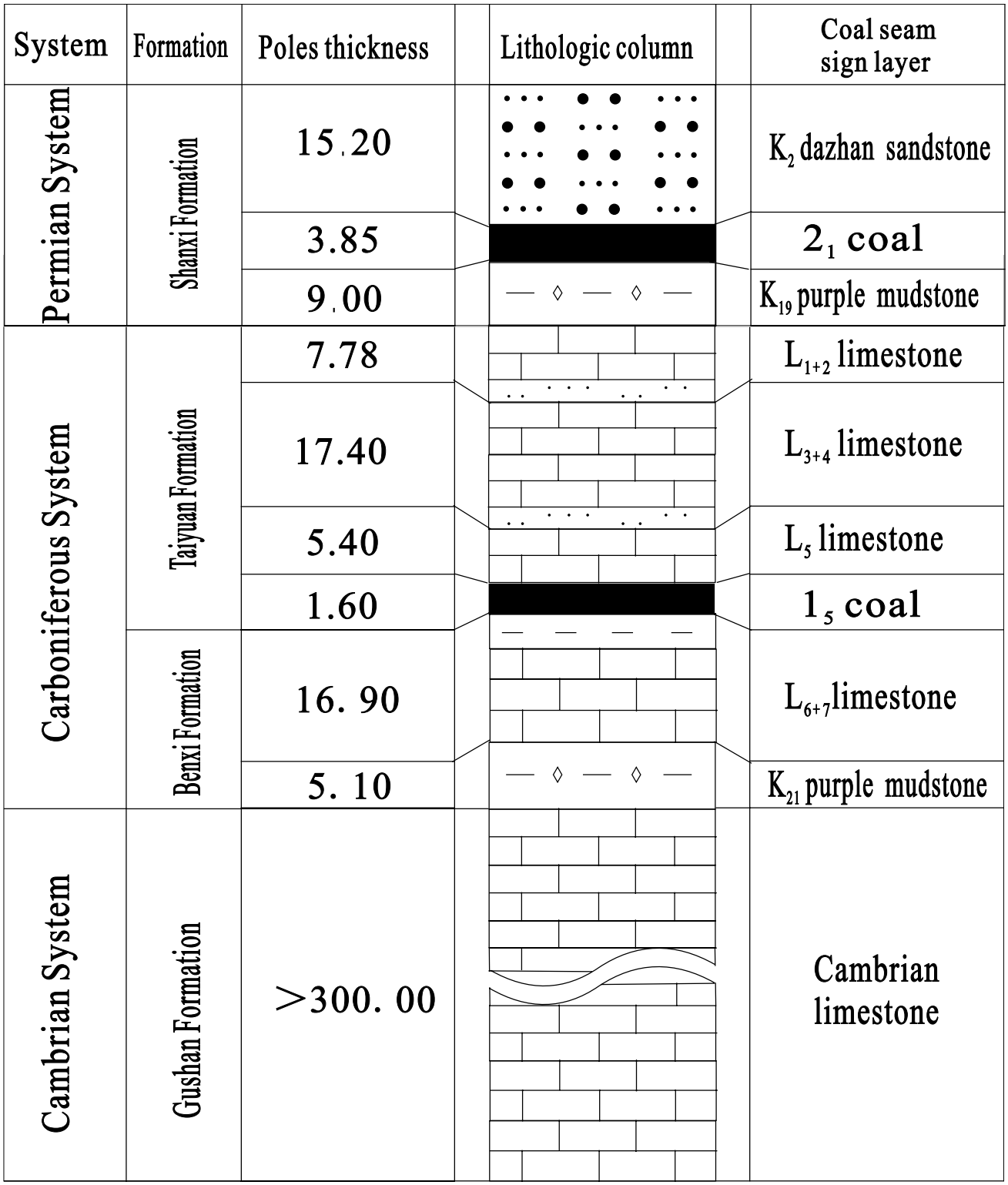

Fig. 2 Columnar schematic diagram of the coal seam overlying the CL

of the mine, at burial depths between 590 and 828 m. By August 2016, the 23,130, F23130, and 23,170 working faces had been completely mined out, while working face 31,010 had advanced 700 m. The plan is to gradually mine working faces 23,150, 23,190, 23,210, 31,030, and 31,050.

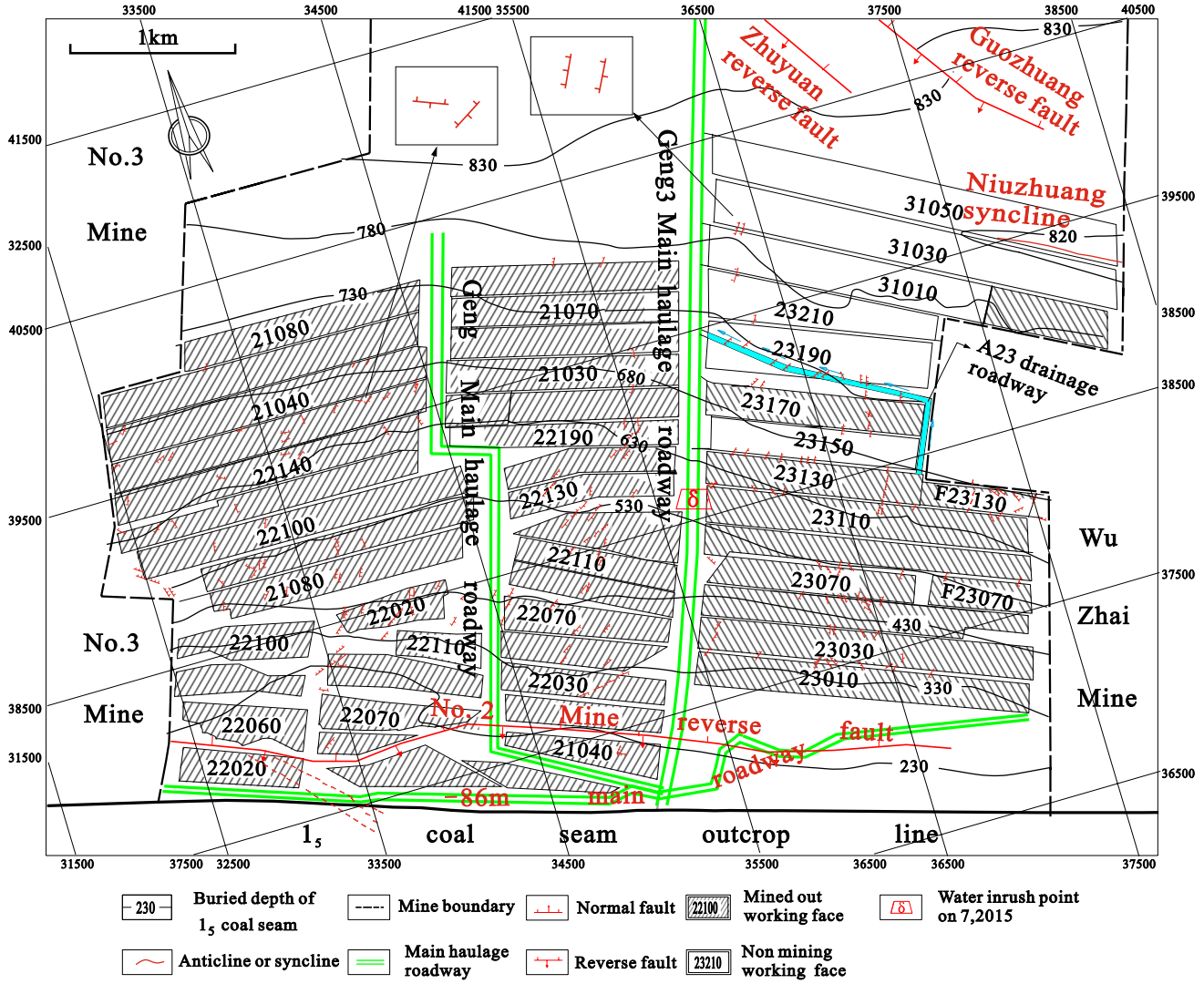

Fig. 3 Mining engineering layout as well as the distribution of the CL in the No. 2 mine

Threatening Aquifers of the 1_5 Coal

The L_5 and L_{6+7} limestone aquifers from the Carboniferous Taiyuan Formation are, respectively, the direct roof and floor aquifers of the 1_5 coal, though the CL beneath the L_{6+7} also indirectly contributes floor water to the 1_5 coal in the No. 2 mine (Fig. 2). The hydrogeological characteristics of the three aquifers are shown in Table 1.

Because the aquifers of the L_5 and the L_{6+7} are all thin, contain relatively little water, and have weak connectivity (less unit inflow and hydraulic conductivity), these aquifers pose only a minor threat to the 1_5 coal mining. In contrast,

Table 1 Water-richness of coal roof and floor aquifers

Aquifer	Average thickness (m)	Average units-inflow (L/(s·m))	Average hydraulic conductivity (m/d)	Water-richness
L_5	5.40	0.114	0.295	Low
L_{6+7}	16.90	0.357	0.189	Low
CL				
Burial depth < 420 m	> 300	4.861	7.470	High
Burial depth > 420 m		0.894	1.096	Medium

because the CL is thicker, contains more fluid, and has better connectivity (greater inflow and hydraulic conductivity), the CL (via the L_{6+7}) can also pose a serious threat to the 1_5 coal mining.

Based on borehole data, the CL is widely distributed at the base of the 1_5 coal, and has an average thickness of 300 m. The distance between the floor of the 1_5 coal and the roof of the CL is 22 m, and groundwater pressure in the latter ranges between 0 and 0.60 MPa. The roof of the CL is between − 300 and − 550 m, and it is located at depths between 530 and 870 m for working faces 23,130 and 31,050 (Fig. 4).

Based on accident records for the No. 2 mine, there have been 32 incidents since 1975 of floor inrush from the CL, and on 23 occasions, the inflow rate exceeded 100 m^3/h. The duration time, amount, and hazard of nine inrush incidents with more than 300 m^3/h are shown in Table 2. Thus, it is clear that 1_5 mining is seriously threatened by the CL.

The Pathway of Mine Water Filling

In the No. 2 mine, small, highly oblique faults are extremely common but larger faults do not exist (Fig. 4). These small faults are mainly banded, heterogeneously distributed, and

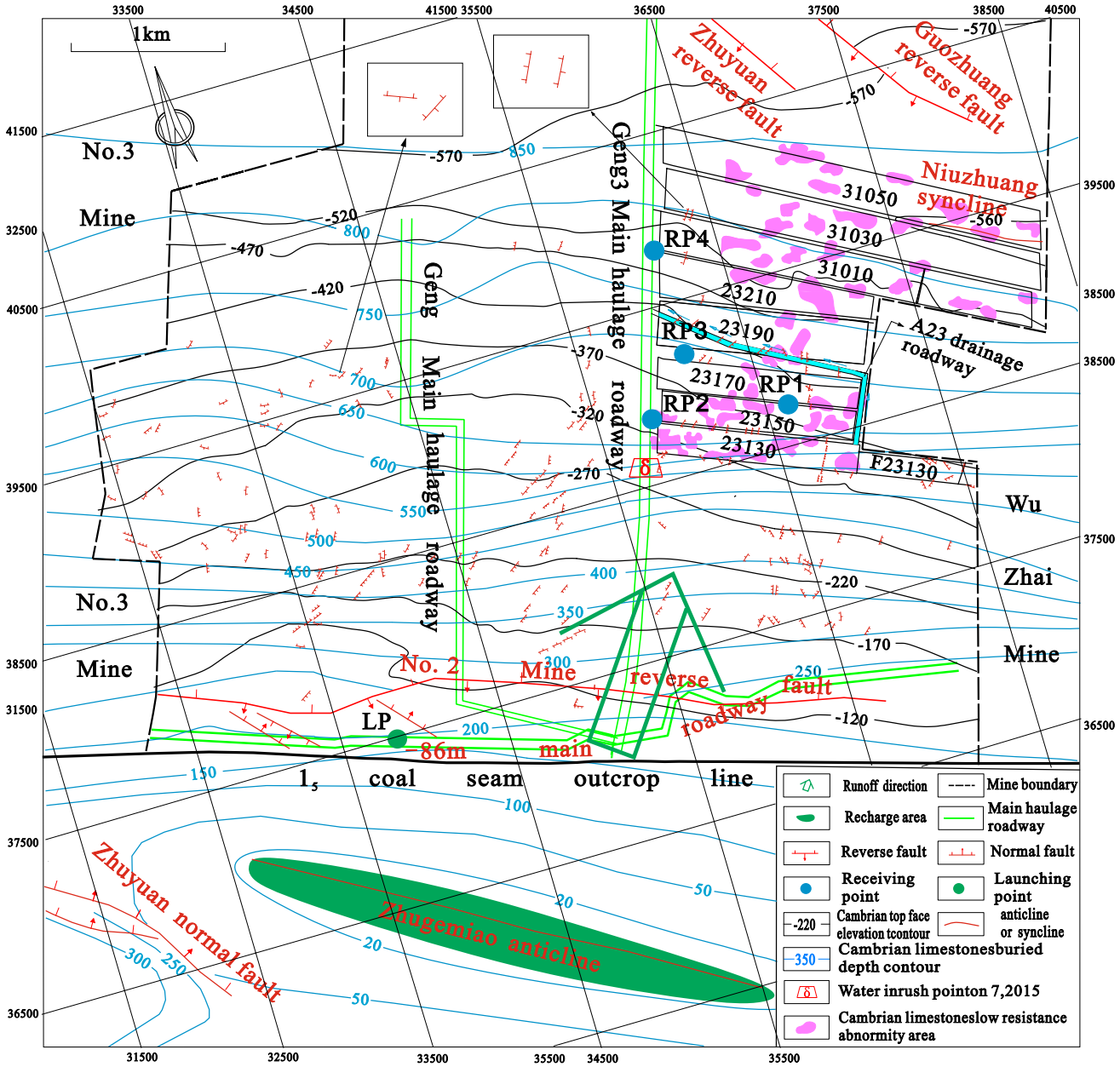

Fig. 4 Buried distributions and underground runoff of the CL in the No. 2 mine

Table 2 Water inrush incidents with more than 300 m^3/h in the No. 2 mine

Date of inrush	Inrush location	Max inflow (m^3/h)	Duration of inrush	Water inrush volume (m^3)	Extent
06.03.1973	Main return air roadway of east wing	716	06.03.1973–05.25.1977	1,174,720	Shut down for 26 days
04.02.1975	131 working face of Ji coal	333	04.02.1975–10.23.1975	36,780	Flooded roadway
05.31.1976	$3^{\#}$ water outlets in return air roadway of Geng coal	504	05.31.1976–01.12.1977	70,620	Flooded roadway
04.01.1977	− 86 m main roadway	1800	04.01.1977–07.26.1977	106,300	Shut down for 17 days
07.24.1977	− 86 m drainage roadway	2000	07.24.1977–03.07.1978	175,200	Shut down for 13 days
11.05.1978	L7 main roadway	556	11.05.1978–09.21.1979	75,840	Flooded roadway
06.03.1981	− 130 m drainage roadway	412	06.03.1981–08.15.1984	115,870	Shut down for 9 days
07.25.2005	$1^{\#}$ water outlets of Geng3 main haulage roadway	2000	07.25.2005–12.02.2010	210,000	Flooded roadway
08.20.2007	$2^{\#}$ water outlets of Geng3 main haulage roadway	450	08.20.2007–12.02.2009.12.2	12,200	Flooded heading faces and unicom lane

have an average density of number 73 per square km (Li et al. 2017b). Because the CL is quite fractured and karst fissures are well-developed, groundwater is abundant and flow channels are common in fault zones. Thus, small faults control the water abundance and groundwater flow characteristics of the CL (Ghasemizadeh et al. 2012; Price et al. 2000; Williams 2008).

The groundwater recharge area of the CL is located within the Zhugemiao anticline (Fig. 4), which leads to a high water pressure threat from below. To counter this, 400 m^3/h is pumped from boreholes that penetrate the CL, to reduce the groundwater hazard in the No. 2 mine.

The Exploration Methods

In order to determine water content and groundwater connectivity of the CL in the No. 2 mine, we used several exploration methods, which included groundwater tracer tests, hydrogeological drilling, groundwater temperature monitoring, and surface transient electromagnetic exploration (TEM).

The CL Groundwater Trace Tests

Two tracer tests were carried out in the No. 2 mine. The time of the first tracer test was between 10:30 a.m. on December 4th and 1:30 p.m. on December 7th, 2013. The second tracer test was from 09:30 a.m. on March 14th until 08:00 a.m. on March 15th, 2014.

An underground geological survey and mapping had demonstrated the presence of a NE-trending fissure belt in the − 86 m main roadway. Because this belt ranges between 30 and 60 cm in width, is very deep vertically, and can be heard to contain flowing water, it was chosen as the launching point (LP) for the tracer test. Four drainage holes were designated as receiving points (RP). LP and RP locations are shown in Fig. 4 and Table 3.

Iodide ion was used as a tracer as this element was undetected in the CL groundwater prior to testing. The potassium iodide concentration released at the LP was 250 mg/L (i.e. the iodide ion concentration was 184 mg/L). To prepare a 250 mg/L potassium iodide solution, an iron container of 2 m^3 was made, filled with distilled water and 500 g of solid potassium iodide, stirred until the potassium iodide fully dissolved, and poured into the delivery point quickly. After the tracer was injected into the LP, the 500 mL water sample was collected at the receiving point every 2 h in the first test, and every 1 h in the second test. 211 water samples were collected during the two tests, and were sent to the Environmental Laboratory of Henan Polytechnic University for iodide analysis using ICS-1100 ion chromatography system. Tracer concentrations at the RPs as well as travel times from the LP to RPs are presented in Table 4.

Hydrogeological Drilling

In order to reduce the pressure of the CL groundwater and ensure safe production, a series of boreholes were drilled in the working face alleys and the A23 drainage roadway. In all cases, the depth of the boreholes entering the CL exceeded 1.5 m. Values for groundwater inflow

and pressure differed in the various drainage boreholes (Table 5). Of the 122 layout drainage water boreholes, 78 were inflow boreholes.

Groundwater Temperature Monitoring

The burial depth and water temperature of the outlet were measured for the inflow boreholes and the water temperature data of the − 86 m main roadway was collected. Groundwater temperatures in the CL boreholes, as well as average burial depths of the CL roof, are shown in Table 6.

Surface TEM of the CL

To further assess the water quantities and hydraulic connectivity of the CL, surface TEM was carried out in the mine (Fig. 4). The detection area was 4.91 km^2, and detection depth into the CL was 200 m. The measuring point spacing of the northwest and northeast measuring lines was 20 and 40 m, respectively, with a total of 6,391 physical points. The apparent resistivity of the surface TEM for the CL was 1–180 Ω·m, defining apparent resistivity values less than 30 Ω·m as characteristic of anomalous low-resistivity zones (ALRZ). The ALRZ of the No. 2 mine are shown in Fig. 4.

Table 3 Location and parameters of the LP and RPs

Test point	Location	Water level elevation of CL (m)	Distance to LP (m)	Water surface slope
LP	− 86 m main roadway	− 86	0	
RP1	23,170 air alley	− 395	3,162.54	0.0977
RP2	Intersection of 23,130 air alley and Geng3 main haulage roadway	− 320	2,548.23	0.0918
RP3	23,170 haulage alley	− 400	3,003.81	0.1045
RP4	Intersection of 31,010 air alley and Geng3 main haulage roadway	− 500	3,587.75	0.1154

Table 4 Calculated values of groundwater velocity and hydraulic conductivity

Test point	The first connectivity test				The second connectivity test			
	Concentration (mg/L)	Time (h)	Velocity (m/d)	Hydraulic conductivity (m/d)	Concentration (mg/L)	Time (h)	Velocity (m/d)	Hydraulic conductivity (m/d)
LP	184.03	0			184.03	0		
RP1	0.008	50.00	1518	15,538	0.073	18.50	4103	41,993
RP2	0.376	52.00	1176	12,812	0.007	16.50	3707	40,376
RP3	0.017	45.50	1584	15,162	0.095	17.50	4120	39,421
RP4	0.009	70.83	1216	10,534	0.003	22.50	3827	33,162
Average			1374	13,511			3939	38,738

Table 5 Data from the CL drainage boreholes in working faces

Working face/roadway	Drainage boreholes			Groundwater inflow (m^3/h)			Groundwater pressure (MPa)	
	Total	Inflow	**Ratio** (%)	Single borehole (min–**max**)	Total steady inflow	**Average**	Single borehole (min–max)	**Average**
23,130	27	22	**81.48**	0.01–**80.00**	198.00	**9.00**	0–0.56	**0.20**
F23130	22	13	**59.09**	0.01–**7.00**	12.94	**1.00**	0–0.30	**0.09**
23,170	29	13	**44.82**	0.10–**20.00**	33.30	**2.56**	0–0.52	**0.11**
A23 drainage roadway	8	1	**12.50**	0.50	0.50	**0.5**	0	**0**
31,010	36	29	**80.56**	0.03–**30.00**	31.50	**1.09**	0–0.55	**0.08**

Table 6 Groundwater temperatures measured in the CL boreholes

Roadway or alley	No. of borehole inflows	Average buried depth of CL roof (m)	Groundwater temp. (°C)	
			Single borehole (min–max)	Average
− 86 m main roadway	1	170	25	25
23,130 air alley	16	600	25–26	25.5
23,130 haulage alley	6	660	26–27	26.5
F23130 air alley	7	540	31–33	32.0
F23130 haulage alley	6	580	33–35	34.0
23,170 air alley	4	675	31	31.0
23,170 haulage alley	9	685	32–34	33.0
A23 drainage roadway	1	715	35	35.0
31,010 air alley	24	780	38–41	39.5
31,010 haulage alley	5	815	38–41	39.5

The CL Connectivity and Abundance

Based on the Trace Tests

Based on the data from the two tracer tests, we calculated the CL groundwater velocity (Table 4) using the distance between the LP and RPs, and the tracer travel time. The average values for the two tests were 1,374 m/d and 3,939 m/d, respectively. The velocity of the second test was higher because after a long period of pumping, the conductivity of CL groundwater had increased. Incorporating the water surface slope and the CL groundwater velocity, we calculated hydraulic conductivity (k) values using Darcy's law of 13,511 and 38,738 m/d, respectively (Table 4). Taking previous research into account, the CL can be defined as a pole-strength conductivity aquifer because the calculated values of k exceeded 50 m/d. Indeed, the size of the k values from both tracer tests indicates good CL groundwater connectivity between the LP and RPs. The fact that the tracer concentrations were significantly different between adjacent RPs suggests weaker groundwater connectivity between these sites. Obviously, the k values based on the two tracer tests were very high, which suggests that there are karst underground "rivers" in the area due to the presence of the fracture zones.

Based on the Hydrogeological Drilling

As shown in Table 5, all four indexes (i.e. borehole inflow ratio, maximum groundwater inflow of a single borehole, average steady groundwater inflow, and average groundwater pressure, the bold type in Table 5) that we measured at working face 23,130 falls into the higher value range, indicating good water-bearing and water abundance characteristics. In contrast, values for the F23130 and 23,170 working faces as well as the A23 drainage roadway fell within the lower range of values, suggesting less significant water-bearing and water abundance characteristics. At working face 31,010, the ratio of inflow boreholes was higher than that at F23130, 23,170, and the A23 drainage roadway, which implies enhanced water-bearing capabilities. At the same time, the maximum groundwater inflow of a single borehole, as well as the average values for steady groundwater inflow and water pressure, were all less than that at working face 23,130, suggesting the presence of less water at working face 31,010.

Although working faces F23130 and 23,170 are located close to 23,130, their water-bearing properties and levels of water abundance differ significantly from working face 23,130, indicating that the CL groundwater connectivity between them is weak. In contrast, once a new borehole was drilled into working face 31,010, inflow and water pressure dropped suddenly at the others nearby, indicating enhanced groundwater connectivity at working face 31,030.

Based on the Temperature Monitoring

As shown in Table 6, the average difference in burial depth between the 23,130 working face and the − 86 m main roadway was between 430 and 490 m, while the average temperature difference ranged from 0.5 to 1.5 °C. This shows that CL groundwater connectivity was enhanced between the 23,130 working face and the − 86 m main roadway.

The average depth difference between the air and haulage alleys in working face 23,130 was 60 m, but the average temperature difference was just 1 °C. At the same time, the average depth difference between the air and the haulage alleys of working face 31,010 was 20 m, while the average temperature difference remained the same. These data suggest good CL groundwater connectivity near both the 23,130 and 31,010 working faces.

The average burial depth difference between the air alleys of working faces F23130 and 23,130 was 60 m, while the average temperature difference was 6.5 °C (Table 6). In contrast, the depth difference between the haulage alleys of

these two working faces was 80 m, and their average temperature difference was 7.5 °C (Table 6). The average burial depth difference between the 23,130 haulage alley and the 23,170 air alley was just 15 m, and the average temperature difference was 4.5 °C. These data suggest that there is almost no hydraulic connectivity between the CL groundwater at any of the working faces (i.e. between F23130 and 23,130 or between 23,170 and 23,130).

The average difference in burial depth between the A23 drainage roadway and the haulage alley of working face 23,170 was 30 m, while the average temperature difference was 2 °C. At the same time, the average difference in burial depth between the A23 drainage roadway and the air alley of working face 31,010 was 65 m and the average temperature difference was 4.5 °C (Table 6). The average burial depth difference between the air and haulage alleys of the F23130 working face was 40 m and the average temperature difference was 2 °C, while the average depth difference at the 23,170 working face was 10 m, and the average temperature difference was 2 °C. Because these results differ from the measured location temperature gradient of 3.4 °C/100 m within the No. 2 mine (Cao et al. 2014; Wang et al. 2016a), they indicate that the CL groundwater connectivity is weaker at different locations.

Based on the Surface TEM

The aforementioned results demonstrate that the abundance and connectivity of the CL are both better near working face 23,130. In contrast, at the 31,010 working face, connectivity was enhanced while water was less abundant, while both water abundance and connectivity were weaker at the F23130 and 23,170 working faces and the A23 drainage roadway. To further investigate these phenomena, the ALRZ results from surface TEM were analyzed (Fig. 4). The results of this analysis demonstrate the presence of numerous ALRZ that are continuous at working faces 23,130 and 23,150 (Fig. 4). In contrast, while numerous ALRZ are present at working faces 31,010, 31,030, and 31,050, their continuity is weak. ALRZ are almost absent from working faces 23,170, 23,190, 23,210, and the A23 drainage roadway. There is no evidence at all for an ALRZ at working face F23130. Abundance and connectivity were better adjacent to working faces 23,130 and 23,150, while the CL abundance at 31,010, 31,030, and 31,050 was significant, but connectivity was weaker. Both abundance and connectivity of the CL were weak at working faces F23130, 23,170, 23,190, and 23,210, as well as at the A23 drainage roadway.

Abundance and connectivity results for the CL identified using surface TEM correlate with data from other methods at working faces 23,130, F23130, 23,170, 31,010, and the A23 drainage roadway; this suggests that the use of surface TEM is reliable. Thus, the surface TEM results could be used to prevent CL groundwater-related disasters, at least at future mining working faces 23,150, 23,190, 23,210, 31,030, and 31,050.

Disaster Prevention of the CL Groundwater

The Rules of CL Disaster Prevention in the Pingdingshan Coalfield.

The water inrush coefficient is commonly used to evaluate the inrush potential of coal floor aquifers (State 2009). The water inrush coefficient (λ) is calculated as follows:

$$\lambda = {}^{P}/_{M} \tag{1}$$

where λ is measured in MPa/m; P is the water pressure from below, MPa; and M is the aquiclude thickness of the floor, m (Fig. 5).

In China, when $\lambda \leq 0.06$ MPa/m, there is no possibility of water inrush from floor aquifers, and when $\lambda > 0.06$ MPa/m, the possibility exists (State 2009). For the Pingdingshan coalfield, when $\lambda > 0.06$ MPa/m, the most effective method for preventing water inrush is depressurization using boreholes to drain groundwater (Zhang et al. 2012) to reduce the P value.

In order to improve the effectiveness of the drainage boreholes in the Pingdingshan coalfield, these rules are followed: (1) Based on the hydrogeological characteristics (the connectivity and abundance) of the CL below the working face, underground TEM is carried out in the working face alleys to determine the ALRZ. (2) Drainage boreholes are deployed to reduce the water pressure of the floor aquifers only when $\lambda \leq 0.06$ MPa/m, and the mining activities permit implementation. (3) Real-time monitoring of underground water pressure and timely calculation of λ are carried out to guide the drainage to ensure safe mining of the working face. (4) For mines that may experience inrush from below, contingency plans are developed to minimize water damage losses.

The Measures of CL Disaster Prevention in the No. 2 Mine

Our research has demonstrated that both the amount of water and connectivity of the CL are enhanced in the region of working face 23,150, and that this face is closely connected hydraulically with 23,130. In contrast, while the CL abundance at faces 31,030 and 31,050 is weaker, groundwater connectivity at these sites is better. Both aspects are weak at 23,190 and 23,210. Thus, based on the data from these working faces, we suggest the following preventative measures to mitigate future mining floor groundwater disasters:

First, after the underground roadway is built, underground TEM work should be carried out to determine the ALRZ. Boreholes in the plane should be located in the ALRZ, not

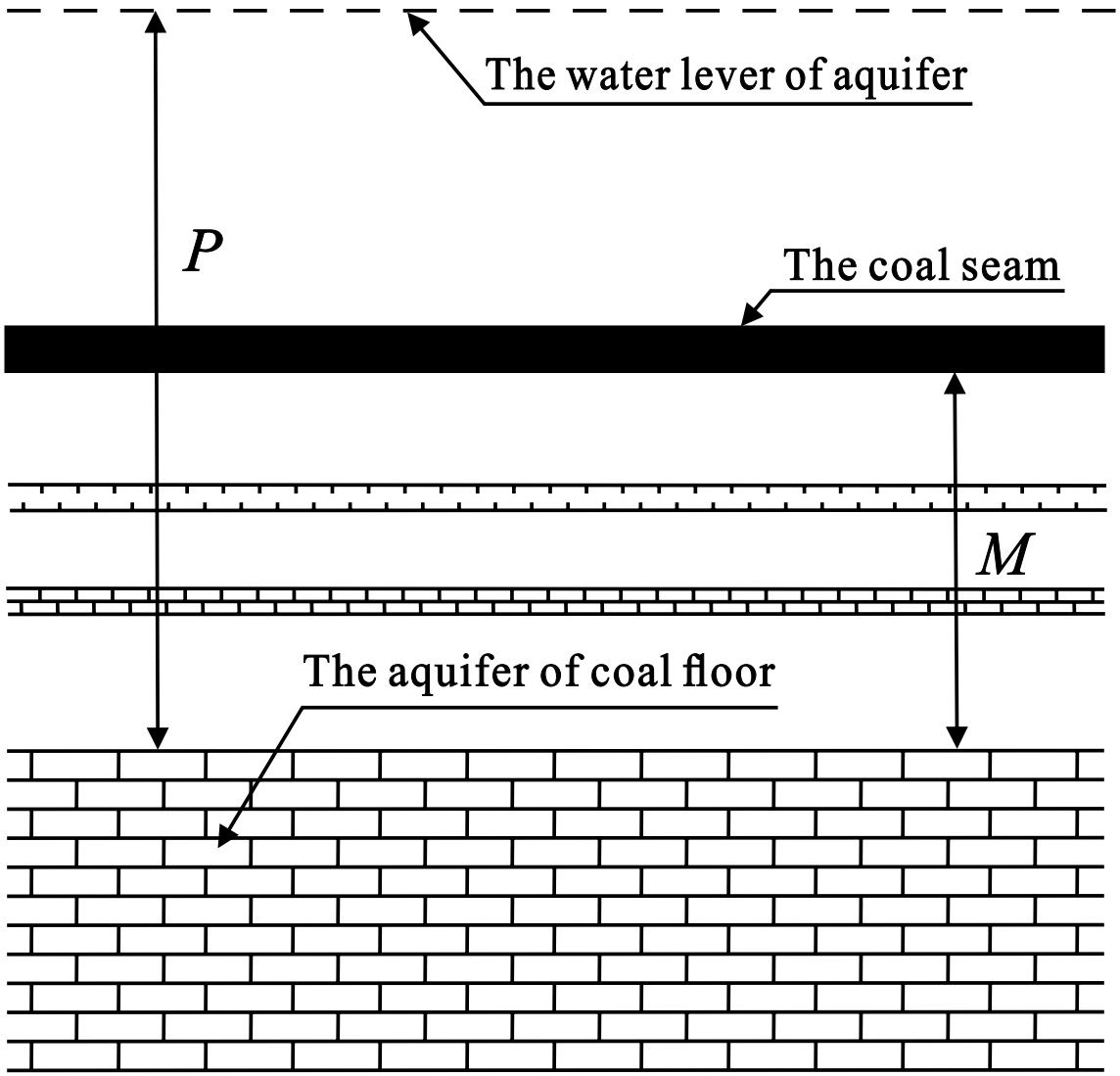

Fig. 5 The relation schema of coal seam and floor aquifer

less than 100 m deep into the CL. Areas with many ALRZ and good continuity require more boreholes.

Second, at the 23,150 working face, drainage will need to be implemented via boreholes in the roadway to working face 23,130 to reduce recharge of the CL groundwater to the 23,150 working face. Drainage boreholes should therefore be drilled into the A23 drainage roadway, penetrating through the 23,150 face to reduce the CL groundwater pressure. At the same time, these measures will need to be monitored and maintained to ensure that flow to the A23 drainage roadway remains unblocked. We recommend that an appropriate discharge system be established and regularly maintained to ensure that there is no seepage in the alleys of the 23,150 working face.

Third, drainage boreholes should be drilled in the air alleys or haulage alleys of working faces 31,030 and 31,050 to reduce the CL groundwater pressure. A discharge system should also be put in place and maintained regularly, again to ensure that there is no seepage in the alleys of working faces 31,030 and 31,050.

Fourth, the inflow at working faces 23,190 and 23,210 will have to be accurately predicted. The drainage system of the working surface is composed of storage tanks, drainage pumps, drainage pipes or drains, and power supply devices; these should be designed and installed based on the expected amount of inflow. During mining, the drainage system will have to be regularly maintained to ensure its continued operation.

Fifth, it is necessary to carry out monitoring work, such as water level, water inflow amount, water quality, and temperature of the CL in real time, and systematically analyze the monitoring data to predict the potential

of mine water damage. And to draw up emergency plans and on-site emergency disposal measures of mine water to minimize the risk of mine production.

Conclusions

Within the No. 2 mine, small faults are extremely common and well-developed, but are heterogeneous in distribution and have an average density of 73/km^2. Groundwater flow channels are well developed within these fault zones; indeed, small faults control both the abundance and runoff of the CL groundwater.

The estimated hydraulic conductivity of the CL aquifers from the two tracer experiments are, respectively, 13,511 m/d and 38,738 m/d, indicating that CL groundwater is very well connected within the experimental area. According to the 4.91 km^2 surface TEM results, apparent resistivity values of less than 30 Ω·m are characteristic of the ALRZ, which can be used to establish water control measures for future mining.

The results of this study show that both the amount of water and connectivity of the CL are enhanced at the 23,150 working face. At the same time, the CL abundance is weaker at working faces 31,030 and 31,050, although groundwater connectivity is better. Both the abundance and connectivity of the CL are weak at working faces 23,190 and 23,210. On the basis of this study, we have outlined a strategy for the prevention of the CL groundwater disasters in future mining working faces. To prevent disasters at the 23,150 working face, drainage of the CL groundwater should be combined with drainage measures at working face 23,130 and the A23 drainage roadway. At the same time, at 31,030 and 31,050, it will be important to drain groundwater in the air alleys or haulage alleys. Finally, establishing appropriate discharge system at working faces 23,190 and 23,210 will be key to preventing future groundwater disasters.

We analyzed the hydrogeological characteristics of the CL using the available materials in the Pingdingshan Coalfield, and recommended corresponding measures to control water damage, providing a reference for similar research in controlling water inrush in coal floors.

Acknowledgements This work was financially supported by the National Natural Science Foundation of China (Grants 41272250 and 41672240), Henan Province's Technological Innovation Team of Colleges and Universities (Grant 15IRTSTHN027), Innovation Scientists and Technicians Troop Construction Projects of Henan Province (Grant CXTD2016053), and the Fundamental Research Funds for the Universities of Henan Province (Grant NSFRF1611). The authors sincerely thank Mr. Jin Yan and Mr. Wenming Lin of the Pingdingshan Tian'an Coal Co. Ltd No. 2 mine for their valuable assistance.

References

Anandan KS, Sahay SN, Ramabadran TK, Shiv PS (2010) Groundwater control techniques for safe exploitation of the Neyveli lignite deposit, Cuddalore district, Tamil Nadu, India. Mine Water Environ 29(1):3–13

Andrea B, Philippe R, Fabien C (2016) Can one identify karst conduit networks geometry and properties from hydraulic and tracer test data? Adv Water Resour 90:99–115

Attila K, Pierre P, Enikő D, László L, Péter S (2015) Well hydrograph analysis for the characterisation of flow dynamics and conduit network geometry in a karst aquifer, Bükk Mountains, Hungary. J Hydrol 530(2):484–499

Cao BQ, Wang XY, Zhang JL (2014) Analysis on temperature distribution and influencing factors in Pingdingshan coal field. Coal Technol 33(7):73–75 [Chinese, with English abstract]

Ghasemizadeh R, Hellweger F, Butscher C, Padilla I, Vesper D, Field M, Alshawabkeh A (2012) Groundwater flow and transport modeling of karst aquifers, with particular reference to the north coast limestone aquifer system of Puerto Rico. Hydrogeol J 20(8):1441–1461

Howladar MF, Deb P, Huqe Muzemder AS (2017) Monitoring the underground roadway water quantity and quality for irrigation use around the Barapukuria Coal Mining Industry, Dinajpur, Bangladesh. Groundw Sustain Dev (4):23–34

Huang PH, Chen JS (2012) Recharge sources and hydrogeochemical evolution of groundwater in the Coal-Mining district of Jiaozuo, China. Hydrogeol J 20(4):739–754

Jing GX, Li DH, Wang XY, Liu XM (2014) Expert interpretation of coal mine safety regulations; relevant laws and regulations of coal mine safety. Provisions on Prevention and Control of Water in Coal Mines. China Univ of Mining and Technology Press, Xuzhou [Chinese]

Lambán LJ, Jódar J, Custodio E, Soler A, Sapriza G, Soto R (2015) Isotopic and hydrogeochemical characterization of high-altitude karst aquifers in complex geological settings. The Ordesa and Monte Perdido National Park (Northern Spain) case study. Science Total Environ 506–507:466–479

Li PY, Hui Qian H, Howard Ken WF, Wu JH (2015) Building a new and sustainable "silk road economic belt". Environ Earth Sci 74(10):7267–7270

Li PY, Wu JH, Qian H (2016) Preliminary assessment of hydraulic connectivity between river water and shallow groundwater and estimation of their transfer rate during dry season in the Shidi River, China. Environ Earth Sci 75:99

Li PY, Qian H, Zhou WF (2017a) Finding harmony between the environment and humanity: an introduction to the thematic issue of the Silk Road. Environ Earth Sci 76:105

Li RZ, Wang Q, Wang XY, Liu XM, Li JL, Zhang YX (2017b) Relationship analysis of the degree of fault complexity and the water irruption rate, based on fractal theory. Mine Water Environ 36(1):18–23

Price M, Low RG, McCann C (2000) Mechanisms of water storage and flow in the unsaturated zone of the Chalk aquifer. J Hydrol 233(1–4):54–71

Qian JZ, Wang L, Ma L, Lu YH, Zhao WD, Zhang Y (2016) Multivariate statistical analysis of water chemistry in evaluating groundwater geochemical evolution and aquifer connectivity near a large coal mine, Anhui, China. Environ Earth Sci 75(9):747

Shi XX, Wu K (2011) Down-hole electromagnetic method for detecting water hazard of coal mine. Proc Environ Sci 11(1):970–976

State Administration of Work Safety in China, State Administration of Coal Mine Safety in China (2009) Provisions on prevention and control of water in coal mines. China Coal Industry Publishing House, Beijing [in Chinese]

Sun WJ, Wu Q, Liu HL, Jiao J (2015) Prediction and assessment of the disturbances of the coal mining in Kailuan to karst groundwater system. Phys Chem Earth 89–90:136–144

Valipour M (2016) How much meteorological information is necessary to achieve reliable accuracy for rainfall estimations? Agriculture 6(4):53

Wang Q, Wang XY, Hou QL (2016a) Geothermal water at a coal mine: from risk to resource. Mine Water Environ 35(3):294–301

Wang XY, Ji HY, Wang Q, Liu XM, Huang D, Yao XP, Chen GS (2016b) Divisions based on groundwater chemical characteristics and discrimination of water inrush sources in the Pingdingshan coalfield. Environ Earth Sci 75(10):872

Wang XY, Wang TT, Wang Q, Liu XM, Li RZ, Liu BJ (2017) Evaluation of floor water inrush based on fractal theory and an improved analytic hierarchy process. Mine Water Environ 36(1):87–95

Williams PW (2008) The role of the epikarst in karst and cave hydrogeology: a review. Int J Speleol 37(1):1–10

Wilson YF (2010) Hydrochemical and isotopic evidence of recharge, apparent age, and flow direction of groundwater in Mayo Tsanaga River Basin, Cameroon: bearings on contamination. Environ Earth Sci 60(1):107–120

Wu Q, Zhao SQ, Dong SN (2013) Mine Water Control Manual. China Coal Industry Publishing House, Beijing [in Chinese]

Yin SX, Zhang JC, Liu DM (2015) A study of mine water inrushes by measurements of in situ stress and rock failures. Nat Hazards 79:1961–1979

Yin SX, Han Y, Zhang YS, Zhang JC (2016) Depletion control and analysis for groundwater protection and sustainability in the Xingtai region of China. Environ Earth Sci 75(18):1246

Zhang JG, Wang LH, Kang GF, Zhang PQ, Song DX, Wang SS (2012) Coal mine limestone water regional governance 2012–2015 plan of China Pingdingshan Coal Group. China Univ of Mining and Technology Press, Xuzhou [Chinese]